Stable gray soliton pinned by a defect in a microcavity-polariton condensate

Ting-Wei Chen,[1] **Wen-Feng Hsieh,**[2] **and Szu-Cheng Cheng**[1,*]

[1]*Department of Optoelectric Physics, Chinese Culture University, Taipei 11114, Taiwan*
[2]*Department of Photonics and Institute of Electro-Optical Engineering, National Chiao Tung University, Hsinchu 30010, Taiwan*

[*]*sccheng@faculty.pccu.edu.tw*

Abstract: We study the spatially localized dark state, called dark soliton, in a one-dimensional system of the non-resonantly pumped microcavity-polariton condensate (MPC). From the recent work by Xue and Matuszewski [Phys. Rev. Lett. **112**, 216401 (2014)], we know that the dark soliton in the pure MPC system is unstable. But we find that a dark soliton pinned by a defect in the impure MPC becomes a gray soliton and can be stabilized by the presence of a defect. Moreover, the stable regime of the gray soliton is given in terms of the defect strength and pump parameter.

OCIS codes: (140.3945) Microcavities; (240.5420) Polaritons; (020.1475) Bose-Einstein condensates; (190.6135) Spatial solitons.

References and links

1. F. Dalfovo, S. Giorgini, L. P. Pitaevskii, and S. Stringari, "Theory of Bose-Einstein condensation in trapped gases," Rev. Mod. Phys. **71**, 463–512 (1999).
2. A. J. Leggett, "Bose-Einstein condensation in the alkali gases: some fundamental concepts," Rev. Mod. Phys. **73**, 307–356 (2001).
3. E. A. Cornell and C. E. Wieman, "Nobel lecture: Bose-Einstein condensation in a dilute gas, the first 70 years and some recent experiments," Rev. Mod. Phys. **74**, 875–893 (2002).
4. W. Ketterle, "Nobel lecture: When atoms behave as waves: Bose-Einstein condensation and the atom laser," Rev. Mod. Phys. **74**, 1131–1151 (2002).
5. D. J. Frantzeskakis, "Dark solitons in atomic Bose-Einstein condensates: from theory to experiments," J. Phys. A: Math. Theor. **43**, 213001 (2010).
6. T. Tsuzuki, "Nonlinear waves in the Pitaevskii-Gross equation," J. Low Temp. Phys. **4**, 441–457 (1971).
7. B. Denardo, B. Galvin, A. Greenfield, A. Larraza, S. Putterman, and W. Wright, "Observations of localized structures in nonlinear lattices: domain walls and kinks," Phys. Rev. Lett. **68**, 1730–1733 (1992).
8. B. A. Kalinikos, M. M. Scott, and C. E. Patton, "Self-generation of fundamental dark solitons in magnetic films," Phys. Rev. Lett. **84**, 4697 (2000).
9. J. Burguete, H. Chate, F. Daviaudand, and N. Mukolobwiez, "Bekki-Nozaki amplitude holes in hydrothermal nonlinear waves," Phys. Rev. Lett. **82**, 3252–3255 (1999).
10. R. Heidemann, S. Zhdanov, R. Sütterlin, H. M. Thomas, and G. E. Morfill, "Dissipative dark soliton in a complex plasma," Phys. Rev. Lett. **102**, 135002 (2009).
11. Y. S. Kivshar, and B. Luther-Davies, "Dark optical solitons: physics and applications," Phys. Rep. **298**, 81 (1998).
12. J. Kasprzak, M. Richard, S. Kundermann, A. Baas, P. Jeambrun, J. M. J. Keeling, F. M. Marchetti, M. H. Szymańska, R. André, J. L. Staehli, V. Savona, P. B. Littlewood, B. Deveaud, and Le Si Dang, "BoseEinstein condensation of exciton polaritons," Nature **443**, 409–414 (2006).
13. H. Deng and Y. Yamamoto, "Exciton-polariton Bose-Einstein condensation," Rev. Mod. Phys. **82**, 1489–1537 (2010).
14. K. G. Lagoudakis, M. Wouters, M. Richard, A. Baas, I. Carusotto, R. André, Le Si Dang, and B. Deveaud-Plédran, "Quantized vortices in an exciton-polariton condensate," Nat. Phys. **4**, 706–710 (2008).
15. J. Keeling and N. G. Berloff, "Spontaneous rotating vortex lattices in a pumped decaying condensate," Phys. Rev. Lett. **100**, 250401 (2008).

#241361 Received 20 May 2015; revised 21 Aug 2015; accepted 23 Aug 2015; published 15 Sep 2015

16. T. W. Chen, Y. L. Chiang, S. C. Cheng, and W. F. Hsieh, "Stability and excitations of spontaneous vortices in polariton condensates," Solid State Commun. **165**, 6–10 (2013).
17. G. Grosso, G. Nardin, F. Morier-Genoud, Y. Léger, and B. Deveaud-Plédran, "Soliton instabilities and vortex street formation in a polariton quantum fluid," Phys. Rev. Lett. **107**, 245301 (2011).
18. A. Amo, S. Pigeon, D. Sanvitto, V. G. Sala, R. Hivet, I. Carusotto, F. Pisanello, G. Leménager, R. Houdré, E. Giacobino, C. Ciuti, and A. Bramati, "Polariton superfluids reveal quantum hydrodynamic solitons," Science **332**, 1167–1170 (2011).
19. R. Hivet, H. Flayac, D. D. Solnyshkov, D. Tanese, T. Boulier, D. Andreoli, E. Giacobino, J. Bloch, A. Bramati, G. Malpuech, and A. Amo, "Half-solitons in a polariton quantum fluid behave like magnetic monopoles," Nat. Phys. **8**, 724–728 (2012).
20. Y. Xue and M. Matuszewski, "Creation and abrupt decay of a quasistationary dark soliton in a polariton condensate," Phys. Rev. Lett. **112**, 216401 (2014).
21. T. Isoshima and K. Machida, "Vortex stabilization in Bose-Einstein condensate of alkali-metal atom gas," Phys. Rev. A **59**, 2203–2212 (1999).
22. M. Wouters and I. Carusotto, "Excitations in a nonequilibrium Bose-Einstein condensate of exciton polaritons," Phys. Rev. Lett. **99**, 140402 (2007).
23. A. Amo, S. Pigeon, C. Adrados, R. Houdré, E. Giacobino, C. Ciuti, and A. Bramati, "Light engineering of the polariton landscape in semiconductor microcavities," Phys. Rev. B **82**, 081301(R) (2010).
24. G. Tosi, G. Christmann, N. G. Berloff, P. Tsotsis, T. Gao, Z. Hatzopoulos, P. G. Savvidis, and J. J. Baumberg, "Sculpting oscillators with light within a nonlinear quantum fluid," Nat. Phys. **8**, 190–194 (2012).

1. Introduction

In the past two decades, the rapid experimental and theoretical developments in the field of Bose-Einstein condensates (BECs) [1–4] have led to a surge of interest in the study of the nonlinear matter waves. The creation of solitary waves in BECs is achievable due to the compensation between dispersion and nonlinearity from particle interactions [5]. The dark soliton (DS) characterized by a density dip and an associated phase gradient can occur in BECs with repulsive interactions. They have been studied [6] and observed in a variety of systems such as discrete mechanical systems [7], magnetic films [8], fluids [9], and plasmas [10]. They have also attracted a great deal of interest in the field of nonlinear optics [11]. DSs occurring in one-dimensional systems are like quantized vortices in two-dimensional systems to show a clear evidence of the occurrence of macroscopic quantum coherence.

In recent years, microcavity-polariton condensates (MPCs) created in semiconductor microcavities [12] have received a great attention. Microcavity-polaritons are bosonic quasi-particles arising from the strong coupling between excitons and photons in semiconductor microcavities. Because of their small effective mass and strong nonlinearity, microcavity-polaritons can condense into a MPC even at the room temperature [13]. Owing to its pump-dissipative character, the MPC is a non-equilibrium system pumped by a laser continuously. The MPC then becomes a good candidate to investigate physical phenomena of the non-equilibrium quantum fluid. By virtue of its non-equilibrium process, the MPC can form quantized vortices [14] or even a vortex lattice spontaneously [15]. There are many experiments and theories on studying the properties of spontaneously formed vortices. The stability of spontaneously formed vortices were studied previously [16]. For a wide range of pump powers, the vortices can exist in a homogeneous MPC without rotation.

Although the properties of spontaneously formed vortices were studied thoroughly, the formation and behavior of DSs in *non-equilibrium* MPCs is much less understood [17–20]. In [20], Y. Xue *et. al* have shown the abrupt decay of a DS in the clean MPC, where no defects exist. Such a disappearance of DSs indicates that there is no stable DS in clean MPCs. There is a similar behavior occurring in atomic condensates. The vortex is unstable in atomic BECs if no rotation and defects exist in atomic BECs. However a vortex pinned by defects becomes stable even without a rotation acting on atomic BECs [21]. Based on vortices being stabilized by defects, we introduce defects into the one-dimensional MPC and try to find the solution of a DS pinned by a defect. The solution is obtained by solving the complex Gross-Pitaevskii equation

#241361 Received 20 May 2015; revised 21 Aug 2015; accepted 23 Aug 2015; published 15 Sep 2015

(cGPE) with a defect. This mean-field model for non-equilibrium MPCs is a generic model of considering effects from pumping, dissipation, potential trap, relaxation and interactions. In this paper, we find that DSs pinned by defects can exist stably and become gray solitons in one-dimensional MPCs.

The present paper is organized as follows. In Sec. 2, we study the dynamics of incoherently pumped MPCs with defects. The steady state of the system, which is subject to a uniform pump power is analyzed. We consider and analyze the steady state of the well-known hyperbolic tangent solution (DS) in the absence of a defect. The DS is proved to be unstable from calculating the Bogoliubov-excitation spectra. In Sec. 3, we introduce a point-like defect into the system, and find the stationary gray solitons pinned by point defects. The stability of gray solitons pinned by point defects is shown in the Bogoliubov-excitation spectra. In. Sec. 4, to check the results from Sec. 3, we change point defects into defects with a finite size. The numerical solutions of gray solitons pinned by finite-size defects are discussed. The stability and Bogoliubov-excitation spectra of gray solitons pinned by finite-size defects are also investigated. Finally, conclusions are given in Sec. 5.

2. The dynamics of microcavity-polariton condensates

In order to study non-equilibrium MPCs, we treat the polaritons at high momenta as a reservoir whose state is determined by the reservoir density, $n_R(r,T)$. Then we employ the generalized cGPE [15, 22], governing the condensate polaritons that couple to the reservoir polaritons, to describe the dynamics of the condensate. The wave function $\Psi(r,T)$ of the condensate and the reservoir density $n_R(r,T)$ satisfy the coupled differential equations written as

$$i\hbar\frac{\partial\Psi}{\partial T} = -\frac{\hbar^2}{2m}\frac{d^2\Psi}{dX^2} + \frac{i}{2}\hbar[R(n_R)-\gamma]\Psi + \tilde{V}(X)\Psi + g|\Psi|^2\Psi + 2\tilde{g}n_R\Psi, \tag{1}$$

$$\frac{\partial n_R}{\partial T} = P - \gamma_R n_R - R(n_R)|\Psi|^2, \tag{2}$$

where X and T are the coordinates for length and time, respectively; γ_R and γ are the decay rates of reservoir and condensate polaritons; g and $\tilde{g}$ are the strength of polariton-polariton interactions and the coupling constant between the condensate and reservoir. $\tilde{V}(X)$ represents the external potential, and $R(n_R)$ is the amplification rate that describes the replenishment of the condensate state from the reservoir state by stimulated scattering. The system is uniformly pumped with a pump power P, which will contribute to the reservoir density.

In the steady state, the reservoir density is $n_R(X,T) = n_R^0$ and the wave function can be described by $\Psi(X,T) = \Psi_0(X)e^{-i\mu T/\hbar}$ with chemical potential μ and Planck's constant $\hbar$. For $P < P_{th}$ (below condensate threshold), there is no condensate density ($\Psi_0 = 0$) and the reservoir density is proportional to the pumping power, i.e., $n_R^0 = P/\gamma_R$. At the threshold, the reservoir density $n_R^{th} = P_{th}/\gamma_R$ is fixed by the balance between the amplification rate $R(n_R(X,T))$ and decay rate γ of the condensate, i.e., $R(n_R^{th}) = \gamma$. When $P > P_{th}$, the condensate appears and the density away from the defect region grows as $n_c = (P_{th}/\gamma)\alpha$, where $\alpha = (P/P_{th}) - 1$ is called the pump parameter being the relative pumping intensity above the condensate threshold. In the mean time, the stationary reservoir density, which is determined by the net gain being zero, is equal to the reservoir density at the threshold pump power, $n_R^0 = n_R^{th}$. Then, the chemical potential of the system is $\mu = gn_c + 2\tilde{g}n_R^0$. Throughout the simulation in this paper, we take $\tilde{g} = 2g$ under the Hartree-Fock approximation [22]. We also choose the length, time and energy scales in units of η, $1/\omega_0$ and $\hbar\omega_0$, respectively, where $\eta = \sqrt{\hbar^2\gamma\sigma/2mgP_{th}}$, $\hbar\omega_0 = \hbar^2/2m\eta^2$, m is the polariton mass and $\sigma = 1/(1-(4\gamma/\gamma_R))$. Thus $X = x\eta$, $T = t/\omega_0$. Rescaling the wave function $\Psi(X,T) \to \sqrt{n_c}\psi(x,t)$ and reservoir density $n_R(X,T) \to n_R^{th}n(x,t)$, the cGPE of

#241361 Received 20 May 2015; revised 21 Aug 2015; accepted 23 Aug 2015; published 15 Sep 2015

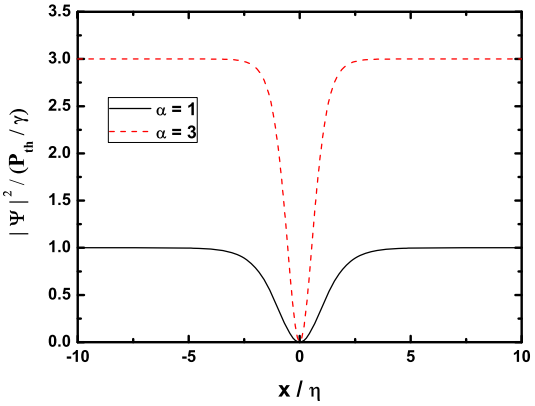

Fig. 1. The density profiles of DSs in a MPC. The black and red-dashed lines are pump parameters $\alpha = 1$ and 3, respectively.

$\psi(x,t)$ and the rate equation of $n(x,t)$ are given as

$$i\frac{\partial \psi}{\partial t} = -\frac{d^2\psi}{dx^2} + \frac{i}{2}[\tilde{R}(n) - \tilde{\gamma}]\psi + V(x)\psi + \alpha\sigma|\psi|^2\psi + (\sigma - 1)n\psi, \tag{3}$$

$$\frac{\partial n}{\partial t} = \tilde{\gamma}_R(\alpha + 1 - n) - 4\tilde{R}(n)\frac{\alpha\sigma}{\sigma - 1}|\psi|^2, \tag{4}$$

where $\tilde{R}(n) = R(n_R)/\omega_0$, $\tilde{\gamma} = \gamma/\omega_0$, $\tilde{\gamma}_R = \gamma_R/\omega_0$ and $V(x) = \tilde{V}(x)/\hbar\omega_0$. The steady state of the system under a uniform pumping can be obtained by substituting $\psi(x,t) = \psi_0(x)e^{-i\tilde{\mu}t/\hbar}$ and $n(x,t) = n_0$ into Eq. (3) and Eq. (4), where $\tilde{\mu} = \mu/\hbar\omega_0$ is the dimensionless chemical potential of the system. Using $\tilde{R}(n) = \tilde{\gamma}$ for the stationary condition, we then have the stationary reservoir density $n_0 = (\alpha + 1 - \alpha|\psi_0|^2)$ from Eq. (4). Therefore, the densities of reservoir polaritons and the condensate are locked together determined by the following time-independent nonlinear equation:

$$\tilde{\mu}\psi_0 = -\frac{d^2\psi_0}{dx^2} + V(x)\psi_0 + \alpha|\psi_0|^2\psi_0 + (\sigma - 1)(\alpha + 1)\psi_0. \tag{5}$$

In the region far away from the center of dark state ($x \to \pm\infty$), the density of the system is uniform with $\psi_0 \to 1$ and $n_0 \to 1$. We then find the chemical potential of the system, $\tilde{\mu} = \alpha\sigma + (\sigma - 1)$, from Eq. (5). Substituting $\tilde{\mu}$ back to Eq. (5), we obtain

$$\frac{d^2\psi_0}{dx^2} + \alpha(1 - |\psi_0|^2)\psi_0 = V(x)\psi_0. \tag{6}$$

In the simplest case, i.e., $V(x) = 0$, one of the solutions of Eq. (6) is a hyperbolic tangent function $\psi_0 = \tanh(Bx)$, where $B = \sqrt{\alpha/2}$. The density distribution of a DS is given by $|\Psi_0|^2 = (P_{th}/\gamma)\alpha(\tanh(Bx))^2$ and is shown in Fig. 1. We see the density notch goes narrower and deeper when the pump power is stronger. The stability of a MPC with or without a defect potential is addressed here by considering linear stability in the framework of the Bogoliubov-de Gennes analysis [22]. We consider small fluctuations $\delta\psi$ and δn acting on the steady state ψ_0 and n_0 of the system.

$$\delta\psi = u_q(x)e^{iqx}e^{-i\Omega t} + v_q^*(x)e^{-iqx}e^{i\Omega t}, \tag{7}$$

#241361 Received 20 May 2015; revised 21 Aug 2015; accepted 23 Aug 2015; published 15 Sep 2015

$$\delta n = w_q(x)e^{iqx}e^{-i\Omega t} + w_q^*(x)e^{-iqx}e^{-i\Omega t}, \tag{8}$$

where u_q, v_q, w_q are the amplitudes of the excitation quasi-particles, and q and Ω are the index labelling the excitation momentum and frequency of the system. For each pump scheme, we get excitation frequency Ω as a function of q. The decay ($\mathrm{Im}(\Omega) < 0$) or growth ($\mathrm{Im}(\Omega) > 0$) behavior of the excitation mode indicates the steady state of the system is stable or unstable, respectively. If the system has one eigenvalue with a positive imaginary part, the corresponding mode will grow exponentially in time identified as a dynamically unstable mode. At the specific $q = 0$, the excitation spectra of DSs without defects is plotted in Figs. 2(a) and 2(b). Moreover, the excitation spectra (the lowest eigenvalues) for all q_s are shown in Figs. 2(c) and 2(d). We consider the situation as [20] has described. A DS in a MPC without defects can be created in a flat pump profile over a large area. There are some modes whose imaginary part of excitation frequencies become positive. This result indicates that DSs without defects in MPCs are unstable. Because there is no particle and repulsive force inside the hole of the DS, excitations can easily redistribute and refill the hole with the MPC density. As time evolved, a sudden collapse of a DS will occur inevitably, which results from the instability of the soliton. This unstable phenomenon is consistent with the conclusion from [20].

3. The stability of a dark soliton pinned by a point defect

In this section, we consider the stationary state of a DS pinned by a point defect at $x = 0$, i.e., $V(x) = V_0\delta(x)$. We take $V_0 > 0$ for a repulsive defect. Such a potential models an impurity which deforms the constant background on a length scale much less than the size of the condensate (or healing length). We can find the analytic solutions of hyperbolic-tangent functions with a localized change in the density around the defect and no oscillations at $x \to \pm\infty$.

The *tanh-mode* solution $\psi_0(x) = \tanh(B(|x| - x_0))$ may exist in Eq. (6), where the translational offset, x_0, is determined by the pump parameter α and potential strength V_0. The dip value of $(\psi_0(x))^2$ is determined by $(\tanh(x_0))^2$, and the density far from the dip is approaching to unity. Integrating Eq. (6) in the vicinity of $x = 0$ results in the following equation

$$\int_{x=0^-}^{x=0^+} \frac{d^2\psi_0(x)}{dx^2}dx = \int_{x=0^-}^{x=0^+} V_0\delta(x)\psi_0(x)dx. \tag{9}$$

This equation can be further simplified into

$$\frac{d\psi_0}{dx}|_{x=0^+} - \frac{d\psi_0}{dx}|_{x=0^-} = V_0\psi_0(0), \tag{10}$$

indicating that the derivative of the wave function experiences a discontinuity at the point defect. After some manipulations, we obtain

$$x_0 = \frac{1}{2B}\sinh^{-1}(\frac{-4B}{V_0}). \tag{11}$$

The x_0 here is negative or positive for the repulsive ($V_0 > 0$) or attractive ($V_0 < 0$) point-defect, respectively. The solution of $\psi_0(x)$ is a dark mode with an envelop having one dip for $V_0 > 0$ while in the case $V_0 < 0$ the envelope has two dips. In this paper we only consider the case $V_0 > 0$ for a repulsive defect and a dark mode with an envelop having one dip. Under the pump parameter $\alpha = 1$ and the potential strength $V_0 = 1$, the wave function as well as the modulus squared one are shown in Fig. 3. The wave function of a DS pinned by a point defect is changing sharply around the pinning site The *tanh-modes* can support a notch density distribution. The dip value of the density distribution is non-zero and given by $(\tanh(x_0))^2$. The DS pinned by a point defect becomes a gray soliton.

#241361 Received 20 May 2015; revised 21 Aug 2015; accepted 23 Aug 2015; published 15 Sep 2015

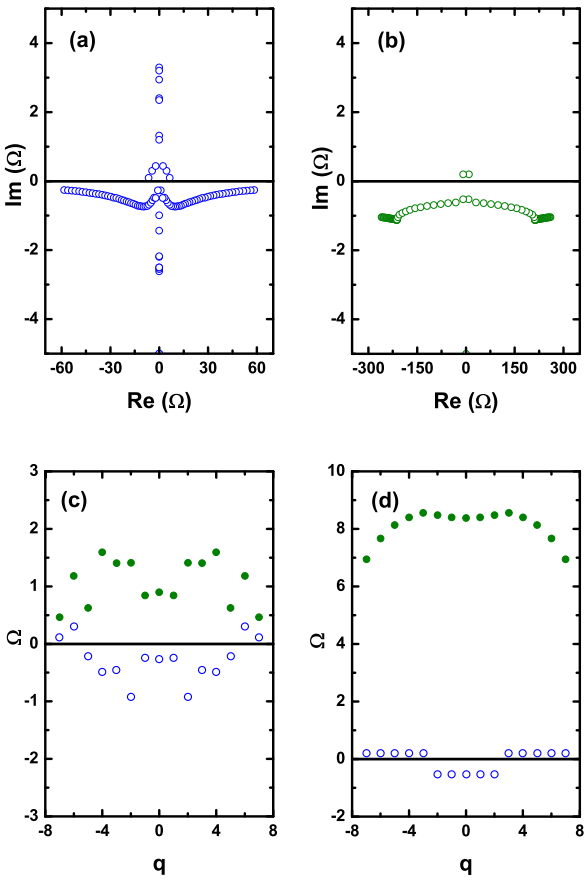

Fig. 2. The Bogoliubov-excitation spectra of the dark soliton in the absence of a defect. (a) $\alpha = 1$ at $q = 0$, (b) $\alpha = 3$ at $q = 0$, (c) $\alpha = 1$ for all q_s, (d) $\alpha = 3$ for all q_s. The solid and empty circles represent the real and imaginary part of the lowest eigenvalues, respectively. The other parameter: $\sigma = 5$.

#241361 Received 20 May 2015; revised 21 Aug 2015; accepted 23 Aug 2015; published 15 Sep 2015

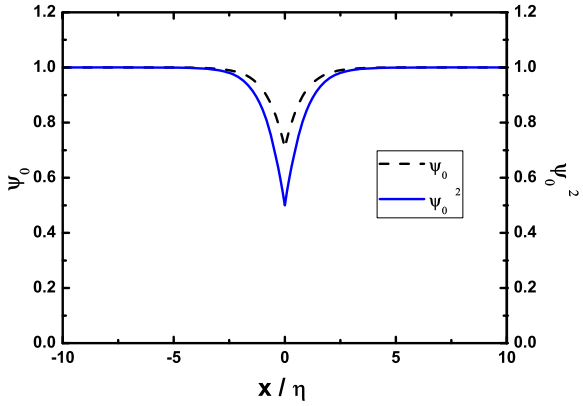

Fig. 3. The wave function $\psi_0(x)$ and its squared modulus $(\psi_0(x))^2$ of the dark soliton pinned by a point defect. This is the case for $\alpha = 1$, $V_0 = 1$.

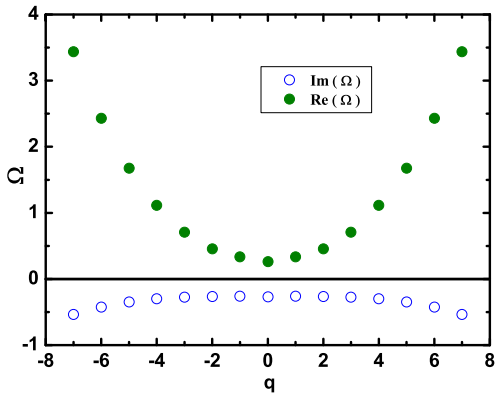

Fig. 4. The Bogoliubov excitation spectrum of the the dark soliton pinned by a point defect. The solid and empty circles represent the real and imaginary part of the eigenvalues, respectively. This is the case for $\sigma = 5$, $\alpha = 1$ and $V_0 = 1$.

After we obtain the analytic wave function of the DS pinned by a point defect, we can check the stability of the gray soliton by perturbing the state. The excitation spectra of the gray soliton are shown in Fig. 4. The excitation energy is increasing with the momentum increasing. The gray soliton is stable as the imaginary parts of excitation spectra are negative. Unlike the DS, a gray soliton has a character that some particles exist in a dip and create repulsive forces to prevent extra particles refilling the dip. In a dip, it is difficult to redistribute the MPC density from excitations. Therefore, the soliton is stabilized by a point defect.

4. The stability of a dark soliton pinned by a finite-sized defect

To check the results shown in Sec. 3, we will study the DS pinned by a defect with a finite size. In the real case, the defect has a finite size. The finite-size effect on pinning and stabilizing

#241361 Received 20 May 2015; revised 21 Aug 2015; accepted 23 Aug 2015; published 15 Sep 2015

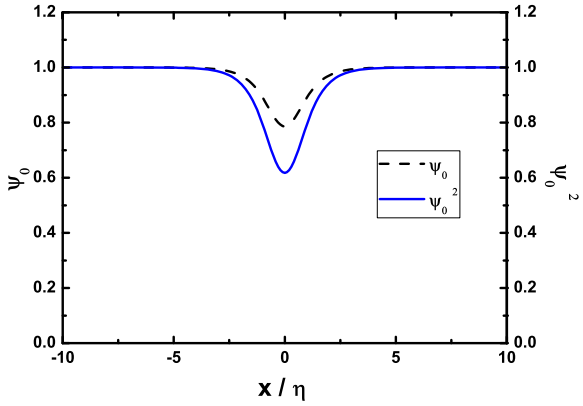

Fig. 5. The wave function $\psi_0(x)$ and its squared modulus $(\psi_0(x))^2$ of the numerical solutions for the repulsive Gaussian-defect using *tanh-mode* as initial iterative solution. This is the case for $\alpha = 1$, $a = 0.5$ and $V_0 = 1$.

the DS is also very interesting. We take a Gaussian distribution with a width a to mimic the finite-size effect of a defect, i.e.,

$$V(x) = \frac{V_0}{\sqrt{2\pi}a} e^{-\frac{x^2}{2a^2}}, \tag{12}$$

where V_0 is the potential strength. There is no analytic solution for Eq. (6) with a Gaussian defect of Eq.(12). We can only integrate Eq. (6) numerically. From the Newton-Raphson method with the initial wave function obtained from the analytical solution in Sec. 3, We then obtain the numerical solution of the DS pinned by a Gaussian defect. The numerical wave function and density distribution of a DS pinned by a Gaussian defect are shown in Fig. 5. Unlike the wave function of a DS pinned by a point defect, the wave function of a DS pinned by a Gaussian defect is changing smoothly around the pinning site. Nevertheless, there is also a notch density distribution. The dip value of the density distribution is also non-zero. The DS pinned by a Gaussian defect becomes a gray soliton, which confirms the results discussed in Sec. 3.

After we obtain the numerical wave function of the DS pinned by a Gaussian defect, we can check the stability of the soliton by perturbing the state. The excitation spectra of the soliton are shown in Fig. 6. The excitation energy is increasing with the momentum increasing. The soliton is stable as the imaginary parts of excitation spectra are negative. The soliton is stabilized by a Gaussian defect. As the potential strength of a Gaussian defect is increasing, we find that the soliton is no long stable. The stable regime of the soliton for the potential strength versus the pump parameter is shown in Fig. 7. The DS pinned by a Gaussian defect can be stable for a wide range of pump parameters as long as the defect potential has a medium strength. The stable regime becomes narrower as the pump power is increasing. There is a maximum strength of the defect potential for the stability of a DS in a fixed pump power. We believe that the nonlinearity is too small to balance the dispersion effect as the pump power is weak. Therefore, a stable DS does not exist even with a defect existing in the system. A formation of the DS becomes possible as the pump power is increasing. But a stable DS has to be pinned by a defect and becomes a gray soliton to prevent excitations from refilling particles in the dip. As the strength of the defect potential is higher, the density of the MPC in a dip of the soliton becomes less. It is easier for excitations redistributing the MPC density in the dip. The stable

#241361 Received 20 May 2015; revised 21 Aug 2015; accepted 23 Aug 2015; published 15 Sep 2015

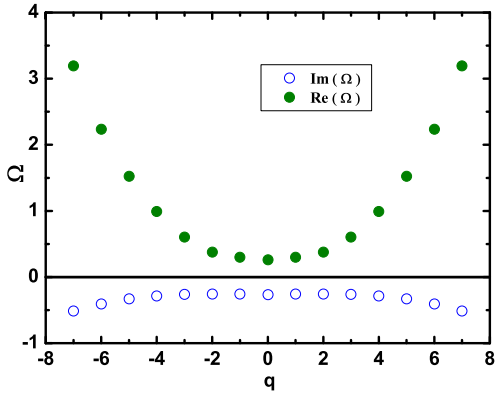

Fig. 6. The Bogoliubov excitation spectrum of the the dark soliton pinned by a Gaussian defect. The solid and empty circles represent the real and imaginary part of the eigenvalues, respectively. This is the case for $\sigma = 5$, $\alpha = 1$, $a = 0.5$ and $V_0 = 1$.

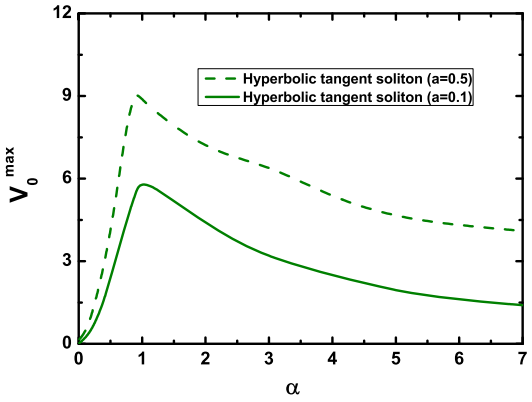

Fig. 7. The maximum Gaussian defect strength (V_0^{max}) in terms of the pump parameter. The widths of the Gaussian potential are $a = 0.1, 0.5$.

#241361 Received 20 May 2015; revised 21 Aug 2015; accepted 23 Aug 2015; published 15 Sep 2015

regime of a DS pinned by a defect is limited by the potential strength of a defect.

We are considering the typical pumping spots, which are much larger than the condensate size or healing length ($\sim 10\mu m$). If we don't shape or focus the laser beam to a smaller size ($< 100\mu m$), then a typical laser emits a beam on the order of $1mm$ in diameter, which can be considered as a homogeneous pumping profile over the condensate. Extra optical confinement achieved by sculpting the pumping profile will create a blue-shift-induced trap from the polariton-polariton interactions in a high-density polariton population [23,24]. Then the boundary condition at $x \to \pm\infty$ in this work is not valid. The polaritons created at lower densities strongly feel this induced potential trap and show strong scattering. In such a spatially modulated pumping scheme [20], the polariton flux exists and the DSs can be spontaneously created through the breakdown of superfluidity. Subsequently, they decay or evolve into other phases due to various instabilities. On the contrary, in this article, we demonstrate that in a nonresonantly pumped *homogeneous* exciton-polariton condensate, the long living DSs are possible to exist by implementing a localized defect.

5. Conclusion

In summary, the stabilization of a DS is addressed by introducing a defect in a non-resonantly pumped MPC. We present an analytical model for a DS pinned by a point defect. A DS pinned by a point defect becomes a gray soliton. From Bogoliubov excitations of the gray soliton, we conclude that the original unstable DS, developed in a spatially homogeneous MPC, becomes stable if there exist a point defect in the system. These results are also computationally demonstrated for a Gaussian defect with a width. We show that the stable regime of a DS pinned by a defect is limited by the potential strength of a defect. There is a maximum strength of the defect potential for the stability of a DS in a fixed pump power.

Acknowledgments

We acknowledge the financial support from the Ministry of Science and Technology of the Republic of China under Contract No. NSC102-2112-M-034-001-MY3 and NSC102-2112-M-009-016-MY3.

#241361 Received 20 May 2015; revised 21 Aug 2015; accepted 23 Aug 2015; published 15 Sep 2015